



Double-orientation code and nonlinear matching scheme for palmprint recognition



Lunke Fei^a, Yong Xu^{a,*}, Wenliang Tang^b, David Zhang^c

^a Bio-Computing Research Center, Shenzhen Graduate School, Harbin Institute of Technology, Shenzhen, China

^b School of Software, East China Jiaotong University, Nanchang, China

^c Biometrics Research Centre, Department of Computing, The Hong Kong Polytechnic University, Hung Hom, Kowloon, Hong Kong, China

ARTICLE INFO

Article history:

Received 25 October 2014

Received in revised form

19 May 2015

Accepted 2 August 2015

Available online 11 August 2015

Keywords:

Biometric

Palmprint recognition

Double-orientation code

Nonlinear angular distance

ABSTRACT

Many palmprint authentication approaches have been proposed in recent years. Among them, the orientation based coding approach, in which the dominant orientation features of palmprints are extracted and encoded into bitwise codes, is one of the most promising approaches. The distance between codes created from two palmprint images is calculated in the matching stage. Reliable orientation feature extraction and efficient matching are the two most crucial problems in orientation based coding approaches. However, conventional coding based approaches usually extract only one dominant orientation feature by adopting filters with discrete orientations, which is sensitive to the noise and rotation. This paper proposed a novel double-orientation code (DOC) scheme to represent the orientation feature of palmprint and designed an effective nonlinear angular matching score to evaluate the similarity between the DOC. Extensive experiments performed on three types of palmprint databases demonstrate that the proposed approach has excellent performance in comparison with previously proposed state-of-the-art approaches.

© 2015 Elsevier Ltd. All rights reserved.

1. Introduction

Biometric authentication is becoming more and more popular because it is an important and effective technology for personal verification and identification [1–4]. In palmprint authentication, the palmprint is defined as the inner surface of a hand. It contains many stable and discriminative features, including not only principal lines and wrinkles but also abundant ridges, minutiae, and textural features [5–7]. Thus the palmprint based authentication approach is able to achieve reliable personal verification and identification. In recent years, the palmprint recognition approach has received increasing research interests and various palmprint recognition algorithms have been presented [8–12] based on different kinds of palmprint features. For example, Huang et al. [13] proposed a principle line based approach for palmprint verification. Dai et al. [14] presented a ridge-based palmprint matching algorithm, which quantitatively investigates the ridge features of high resolution palmprint images and calculates the statistics of ridge features. Morales et al. [15] introduced the scale invariant feature transform (SIFT) based approaches to perform palmprint recognition. The key points of palmprints obtained

using SIFT are that they are robust to the image illumination, scaling and rotation variance. Liu et al. [16] proposed a minutiae-based palmprint matching algorithm based on minutiae clustering and minutiae match propagation. Li et al. [17] designed a palmprint recognition approach based on the fusion of 2D and 3D palmprint features. They first extracted correlated features from 2D and 3D palmprint images. Then, these features were fused at the feature level to achieve satisfactory recognition accuracy. Zhang et al. [18] supplied a multi-spectral palmprint recognition approach which captured palmprint images under red, green, blue, and near-infrared light. These spectral features were combined at the matching score level to improve the performance of palmprint identification. In addition, the subspace based approaches, such as the Principal Component Analysis (PCA) and Linear Discriminant Analysis (LDA) [7–9], and the Representation Based Classification (RBC) approaches, such as CRC [19] and TPTSSR [20], can also be exploited for palmprint authentication [21].

Besides the above approaches, orientation based coding approaches are deemed to be the most promising palmprint recognition approaches, since the palmprint is full of line and textural features which carry rich and distinctive orientation information. Zhang et al. [22] proposed an effective Palmcode approach that applied a normalized 2-D Gabor filter to the palmprint image and encoded the filter results as code representation. Inspired by the Palmcode approach, Kong et al. [23] proposed the Competitive code approach which adopted six

* Corresponding author. Tel.: +86 13640997970; fax: +86 260322461.

E-mail addresses: flksxm@126.com (L. Fei), laterfall@hitsz.edu.cn (Y. Xu), wltang@ecjtu.jx.cn (W. Tang), csdzhang@comp.polyu.edu.hk (D. Zhang).

Gabor filters to extract the dominant orientation features of palmprints based on the principle of the biggest response. Similar to Competitive code method, the Robust Line Orientation Code method (RLOC) [24] extract orientation by using a Modified Finite Radon Transform (MFRAT). Based on the idea of the Competitive code, Zuo et al. [25] designed a novel Sparse Multiscale Competitive Code (SMCC) approach to extract more accurate orientation features by using a bank of multiscale Gabor filters and employing a winner-take-all rule. Subsequently, Kong et al. [26] proposed a fusion code approach that encoded the phase with dominant magnitude from four orientation's Gabor filter results. Sun et al. [27] employed three groups of orthogonal Gaussian filters to extract three binary codes, i.e. the ordinal code, in terms of the sign of the filter results. To further extract more orientation features, Guo et al. [28] proposed a Binary Orientation Co-occurrence Vector (BOCV) approach, which obtained all six orientations by convolving the palmprint image with six Gabor filters and encoded all filter results as orientation features. Zhang et al. [29] had improved the BOCV to E-BOCV by making out the fragile bits to further improve the performance of palmprint recognition.

It is well known that the winner-take-all rule, which extract the single orientation with the largest filter response [23], is usually used in the orientation based coding methods. However, in real operations, a bank of Gabor filters with discrete orientations is used to convolve with palmprint. It is possible that no any filter that has the same orientation as palmprint line and no filter can achieve the absolute maximum of filter response. Actually, the palmprint line usually coincides with two filters, which have larger responses than other filters in most conditions. So double-orientation feature with top-two largest responses is more reasonable than the single-orientation extraction, and it is robust to the noise and rotation.

In this paper, a robust double-orientation code (DOC) approach for palmprint recognition is proposed. First, the paper studies the rationale of the palmprint orientation based coding theory and concludes that the DOC is highly reliable and reasonable for palmprint orientation feature representation. Second, the paper presents an effective nonlinear angular matching score metric for the similarity evaluation of DOC. Finally, extensive experiments on three types of palmprint databases are performed to examine the effectiveness of the proposed approach. The extensive experimental results show that the proposed approach can achieve higher verification and identification accuracy than conventional state-of-the-art coding algorithms.

The remainder of this paper is organized as follows: Section 2 briefly describes the main orientation based coding approaches. Section 3 presents the analysis of the double-orientation extraction. Section 4 introduces the double-orientation code based nonlinear matching scheme for palmprint recognition. In Section 5, experiments of the proposed approach are supplied and analyzed. Finally, Section 6 offers the conclusion of this paper.

2. Related works

2.1. Principal line based approach

Palmprint lines are the basic feature of a palmprint, and line based recognition approaches play an important role in palmprint authentication. The principal line based approaches use a line or edge detector to extract the palmprint lines and then use them to perform palmprint recognition. In general, palms have three principal lines which are the most evident lines in the palmprint image and have stable shapes and positions. Thus the principal lines are highly robust to noise and illumination. Palmprint principal lines can be extracted by using the Gabor filter, Radon filter, Sobel operation. Fig. 1 shows some principal line images extracted by using MFRAT approach [13].

In the matching stage, the similarity is simply evaluated in terms of the number of the overlapping pixels of two palmprint principal lines. A recommended matching approach of principal lines is the pixel-to-area [14] matching approach, which calculates the principal line matching score as follows:

$$S(A, B) = \sum_{i=1}^m \sum_{j=1}^n A(i, j) \cap \bar{B}(i, j) / N_A, \quad (1)$$

where A and B are two palmprint principal line images, “ \cap ” represents the logical “AND” operation, N_A is the number of pixel points of A , m and n are the row number and column number of the palmprint image, and $\bar{B}(i, j)$ represents a neighbor area of $B(i, j)$. The larger the matching score means the greater similarity between A and B .

The principal lines are one of the most stable features of a palmprint. However, using only principal lines is not adequate to represent the uniqueness of a palmprint because different individuals may have similar principal lines. Thus, the recognition accuracy may be low. Moreover, simple using principal line means that many discriminative minutiae are discarded.

2.2. Coding based approaches

In addition to the principal line based approach, the coding based approaches are the most promising methods for palmprint recognition. One or several filters are used to extract palmprint orientation features and these features are then converted into codes. The distance between codes is calculated to perform palmprint recognition. The representative coding based approaches include the Competitive code, Palmcode, Ordinal code, Fusion code, RLOC, BOCV, and E-BOCV approach, and so on.

The Competitive code approach [23] is one of the most popular coding based approaches. Six Gabor filters with different orientations are used to extract orientation features from a palmprint. The orientations are finally determined as $j\pi/6$, where $j = \{0, 1, \dots, 5\}$. Six orientation's Gabor templates are convoluted with the palmprint

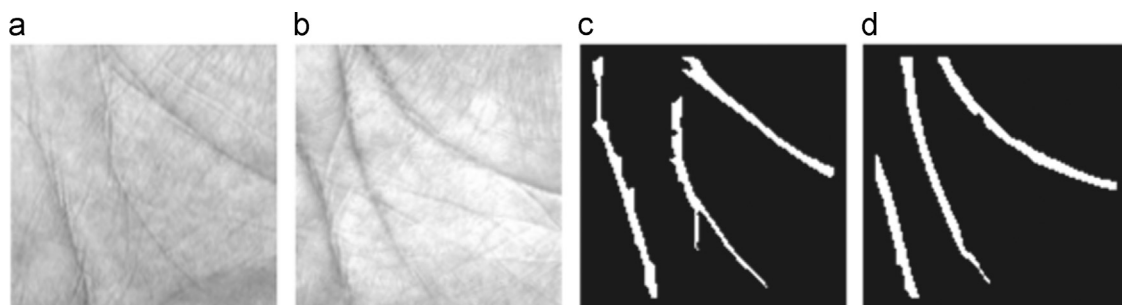


Fig. 1. Palmprint images and their principal line images: (a), (b) are two palmprint images from two subjects and (c), (d) are palmprint principal line images of (a), (b).

image. The final orientation is the orientations with the greatest response principle. It takes the orientation index $j(j=0, 1, \dots, 5)$ as the competitive code. The angular distance metric is used for comparing two competitive codes. The angular distance is based on the following rules: the distance between parallel orientations is 0, the distance is 1 when the angles of the two orientations are $\pi/6$ or $5\pi/6$, the distance is 2 when the angles of the two orientations are $2\pi/6$ or $4\pi/6$, and the distance between perpendicular orientations is 3. For effective calculation, the index competitive code can be represented by three binary codes via the rule in [23]. Then the hamming distance can be used to measure the similarity between two competitive codes:

$$D(P, Q) = \frac{\sum_{y=0}^N \sum_{x=0}^N \sum_{i=1}^3 (P_i(x, y) \cap Q_i(x, y))}{3N^2}, \quad (2)$$

where $P_i(Q_i)$ is the i th bit binary code plane and “ \cap ” is the logical “AND” operation. The value of hamming distance representatives the similarity between two code plane.

Compared with the competitive code approach, the palmcode approach [22] uses only the optimal 2D Gabor filter with orientation of $\pi/4$, including the real part and the imaginary part, to extract palmprint textural features. The fusion code approach [26] uses four complex Gabor filters with orientations of $j\pi/4(j=0, 1, 2, 3)$ to extract palmprint orientation features. The phase with the largest response magnitude of the four filters is converted into a pair of binary codes. The similarity between palmcode and fusion codes is calculated by using the normalized hamming distance. In order to obtain more orientation information, the BOCV approach [28] uses the same six Gabor filters as in the Competitive code approach to convolve with palmprint image. All six orientation features are encoded into six codes, which are joined to calculate the hamming distance between the testing image and training image. Zhang et al. [29] extended the BOCV to E-BOCV by incorporating fragile bits information. In the E-BOCV, fragile bits in BOCV are extracted and excluded from the BOCV matching. And a code map based metric is designed for the fragile bits similarity evaluation, which is fused with BOCV matching in score level fusion.

Similar to the Competitive code approach, the robust line orientation code (RLOC) approach [24] adopts the MFRAT instead of Gabor filter to extract orientation code. The RLOC encodes a pixel as 1 when it is in a certain principal line; otherwise, the RLOC encode the pixel as 0. The pixel-to-area rule is used for the RLOC matching.

Inspired by the ordinal measurement, Sun et al. [27] proposed the Ordinal code approach, which uses three groups of integrated perpendicular 2D Gaussian filters to convolve with palmprint image. The signs of filtering results are encoded into three ordinal codes, and the sum of three bitwise hamming distances is computed for the similarity evaluation between the query and gallery palmprint.

Both Competitive code and Fusion code methods extract the single-orientation base on the rule of winner-take-all [23] that extract the orientation of filter that has the largest filter response with palmprint. The rule of the orientation extraction in the RLOC method is also similar with that of the Competitive code method. It based on the theory that the filter response will reach the maximum when the filter orientation is consistent with that of the palmprint line. However, in real operations, the adopted orientations of filters are discrete. It is possible that no any filter has the orientation of the palmprint line and has the absolute largest response in most conditions. So the single-orientation extraction based on the winner-take-all rule may be unstable. This motivated us to explore a more reasonable orientation based coding approach.

3. Double-orientation feature extraction

The orientation based coding approaches usually based on the assumptions that each pixel in palmprint belongs to a line and the filter response will reach the maximum when the orientation of the filter is consistent with the line orientation [15]. However, in real operations, the orientations of filters are discrete. So the orientation of filters is not exactly consistent with the line orientation in most conditions. This means that the “winner-take-all rule” may not extract the orientation feature correctly.

To investigate the stability of the “winner-take-all rule”, six Gabor filters with orientations of $j\pi/6(j=0, 1, \dots, 5)$ were chosen to perform convolution with palmprint images. Then the top-two responses, i.e. the largest response and the second-largest response, were compared. Palmprint images were selected from the PolyU palmprint database and the multispectral databases, which will be introduced in detailed in next section. In each database, 100 palmprint images from different palms were selected and each image was normalized to 64×64 . There were 4096 pixels in one image and $4096 \times 100 = 409,600$ pixels in 100 images. Each pixel was convolved with six Gabor filters and the discrepancy between top-two largest responses was calculated. The distribution of discrepancy is shown in Fig. 2(a). The x -axis is the pixel distribution and the y -axis represents the top-two largest response discrepancy. It was found that there are many points having very similar top-two largest responses.

The discrepancy-ratio, which is the ratio of the discrepancy to the largest response, was introduced to represent the close degree between the top-two responses. A smaller discrepancy-ratio means a higher similarity between two largest responses. Fig. 2(b) and (c) shows the distribution of the “pixel percentage” and “percentage-summation” with the discrepancy-ratio of PolyU palmprint database. Fig. 2(d) shows the “percentage-summation” distributions on four spectral palmprint databases. The curve in Fig. 2(d) shows that the discrepancy-ratios are smaller than 0.1 for about 50% of pixels and smaller than 0.05 for about 30% of pixels. This means that a large number of pixels have very close top-two responses.

Fig. 3(a) shows a palmprint image and (b) shows the distribution of the pixel whose “discrepancy-ratio” is smaller than 0.02. One pixel is selected to convolve with six Gabor filters and the results of six filters are also shown in the figure. The largest responses is 2.9018 corresponding to an direction of $\pi/6$. Then we add only 0.02% “salt & pepper” noise in the palmprint image. It can be found that the largest response of the pixel changes to 2.9102 with direction of 0 as shown in Fig. 3(c). This indicates that the orientation of the largest response is changed after little noise is imposed. Furthermore, Fig. 3(d) shows that one area of the palmprint image (a) is rotated by 3° of counter-clock. The largest response of the pixel marked in the figure is 4.2523 with a direction of $\pi/6$ before the rotation, and it becomes 4.2525 with a direction of $\pi/3$ after the rotation. Thus, the single-orientation based on the rule of the largest filter response is sensitive to the noise and rotation.

The single orientation of filter that has the largest filter response will be treated as the orientation feature of palmprint in several orientation based coding approaches. This is deemed to be reasonable because of the fact that the filter response will reach the maximum when the filter orientation is consistent with the orientation of palmprint line. However, it is possible that no any filter has the exactly consistent orientation with palmprint line and no filter can achieve the exact maximum of filter response in most conditions. Because only limited discrete orientations (in most approaches there are six orientations) of filters are adopted in real operations. Actually, the palmprint line usually coincides with two filters, as shown in Fig. 4, which usually have larger responses than other filters. In other words, for orientation extraction by using

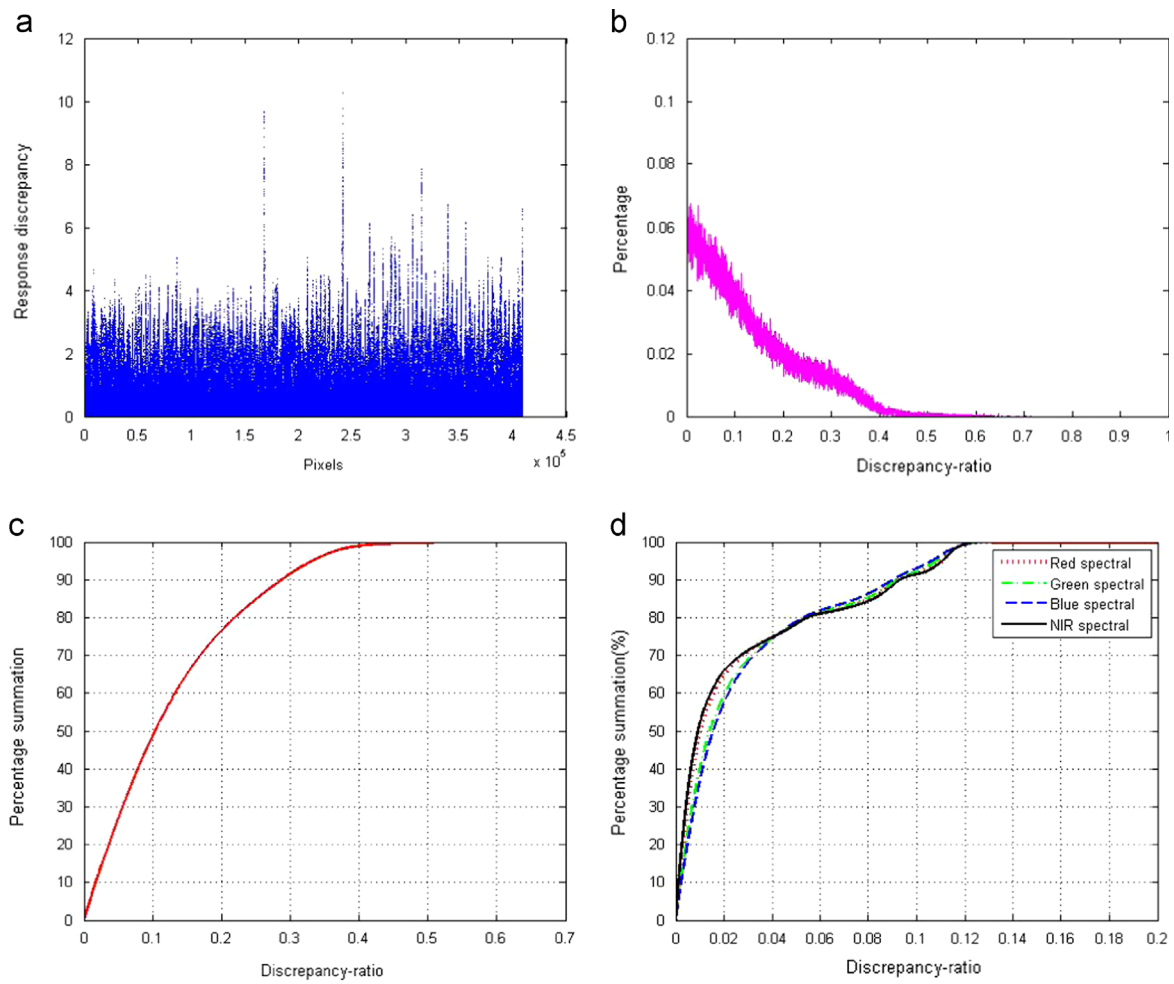


Fig. 2. Top-two response distributions on PolyU palmprint database: (a) and (b) are the largest two response distributions, respectively; (c) is the discrepancy of the top-two responses; and (d) and (e) are the percentage and percentage-summation distributions with the discrepancy-ratio, respectively.

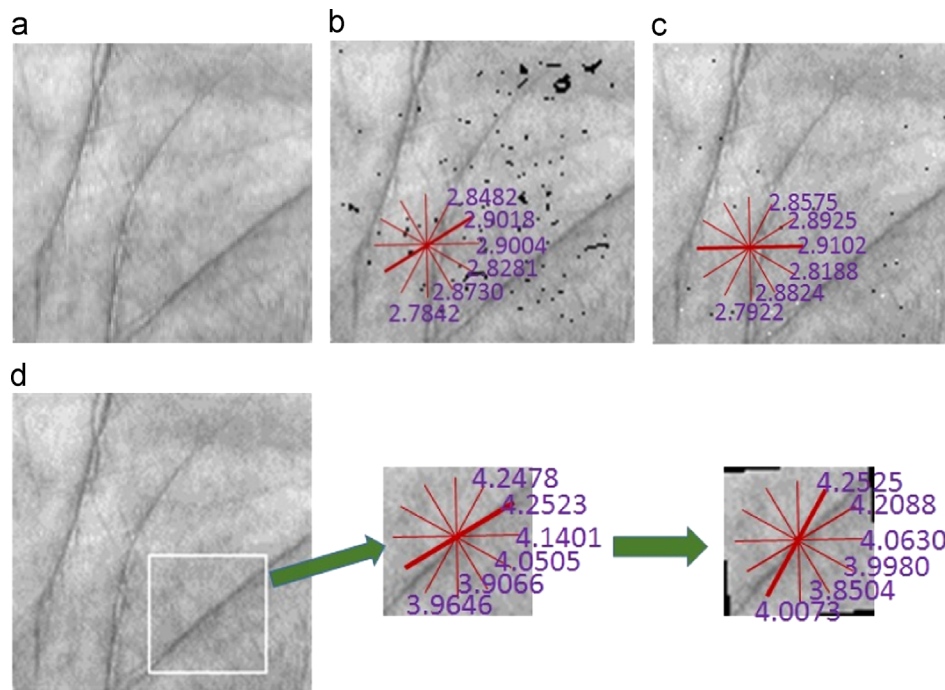


Fig. 3. The top row shows the effect on the response of the noise: (a) is the original palmprint image; (b) depicts the filter responses of one pixel whose "discrepancy-ratio" is less than 0.05; (c) depicts the filter response of the pixel after 0.02% noise is added to the palmprint image (a); and (d) depicts the change of largest response caused by the rotation.

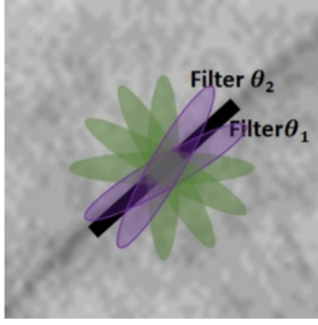


Fig. 4. The palmprint line usually coincides with two filters in most conditions.

discrete orientations of filters, the most possible orientation of palmprint line usually coincide with two orientations of filters and the use of a single filter cannot well model it. Therefore, the double-orientation feature extracted based on the top-two responses should be more reasonable than the single-orientation extraction. Moreover, the double-orientation feature with top-two responses, which is stable even there is little noise or rotation in the palmprint, is more robust than single-orientation.

4. Double-orientation crossing matching scheme

Filter-based approaches are widely used to perform feature extraction of a palmprint such as principal line extraction, texture orientation abstraction and edge detection. Generally there are three kinds of filters, i.e. Gabor filter, Random filter, Gaussian filter [2], and Riesz transform [30], which are usually used for the extraction of palmprint orientation features. Each filter has its own advantages. Of them, the Gabor filter is widely used for extracting orientations or edge information from images [31,32]. Xue et al. [33] compared the performance of the coding based palmprint recognition approaches by using different filters and concluded that the Gabor filter has better performance than other filters. Furthermore, the Gabor filter has good properties of the 2-D spectral specificity of texture as well as its variation with 2-D spatial position. We used the Gabor filter to extract orientation features of palmprint in our approach.

4.1. Revised Gabor filter

The Gabor filter has the following general form:

$$G(x, y, \theta, \mu, \sigma, \beta) = \frac{1}{2\pi\sigma\beta} \exp\left[-\pi\left(\frac{x'^2}{\sigma^2} + \frac{y'^2}{\beta^2}\right)\right] \exp(i2\pi\mu x'), \quad (3)$$

where $x' = (x - x_0) \cos \theta + (y - y_0) \sin \theta$, $y' = (x - x_0) \sin \theta + (y - y_0) \cos \theta$. (x_0, y_0) is the center of the function, μ is the radial frequency in radians per unit length, θ is the orientation of the Gabor function in radians, and σ and β are the standard deviations of the elliptical Gaussian along x and y axis, respectively. The ranges of x and y are the sizes of the filter and $i = \sqrt{-1}$. Similar to the Competitive code approach, the real part of the Gabor filter is applied to extract the orientation feature of the palmprint. The Gabor filter response at an orientation can be treated as confident features occurring at that orientation [32]. Lines are a small-scalar part of the palmprint image [22]. So the real part of the Gabor filter should be transferred to “upside-down” form for more accurate orientation feature extraction. So the largest response means the lowest convolved value. The transformed Gabor filter is defined as

$$\tilde{G} = \frac{1}{2\pi\sigma\beta} \left\{ 1 - \exp\left[-\pi\left(\frac{x'^2}{\sigma^2} + \frac{y'^2}{\beta^2}\right)\right] \cos(2\pi\mu x') \right\}. \quad (4)$$

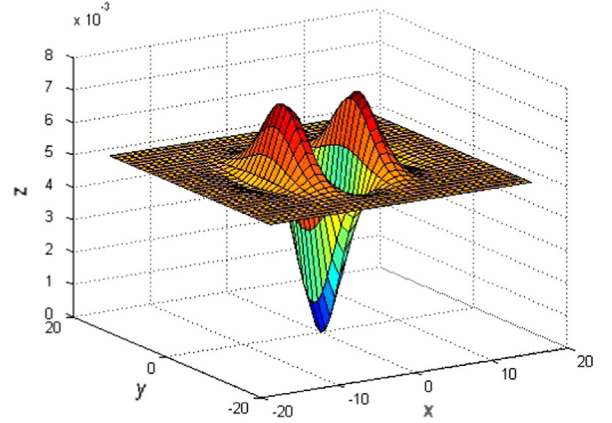


Fig. 5. The appearance of the revised Gabor filter with orientation of $\theta=0$.

A set of optimal parameters are set in the Gabor filter according to [13]. These parameters are $\mu=0.0916$, and $\sigma=\beta=5.6179$. θ is $j\pi/n_\theta$ ($j=0, 1, \dots, n_\theta-1$), where n_θ , which is usually even, is the orientation number used in the adopted Gabor filters. n_θ is set to 6 in this paper generally. Fig. 5 shows the appearance of the revised Gabor filter with orientation $\theta=0$. The revised Gabor filters are used to perform orientation feature extraction of the palmprint image.

4.2. Palmprint preprocessing

All palmprint images are preprocessed before palmprint recognition. This step extracts the central region of a palmprint for accurate matching. In our method, the most representative method proposed in [22] is employed to extract the Region of Interest (ROI) of a palmprint. This method uses gaps between fingers as reference points to determine the ROI of a palmprint. At first, we use the low-pass Gaussian filter to convolve the original palmprint image to convert the convolved image into a binary image by thresholding. Then, we obtain boundaries of the binary image using a boundary tracking algorithm and extract the landmarks based on the boundaries, where the landmarks are at the bottom of gaps between index and middle fingers and between ring and little fingers. Third, we locate the perpendicular bisector of the line segment between two landmarks to determine the centroid of the palmprint region. Finally, we extract the normalized subimage of a fixed size, i.e. 64×64 , as the ROI, which is located at a certain area of a palmprint and used for the palmprint feature extraction. Fig. 6 shows a procedure of the ROI extraction of a palmprint image.

4.3. Double-orientation extraction algorithm

The revised Gabor filters are used to extract double-orientation feature for all pixels in the palmprint image. Let \tilde{G}_j be the \tilde{G} with orientation of $j\pi/n_\theta$, where $j = \{0, 1, \dots, n_\theta-1\}$ and n_θ is the number of Gabor filters. \tilde{G}_j ($j = 0, 1, \dots, n_\theta-1$) are employed to convolve each pixel of the palmprint image:

$$R_j(x, y) = \tilde{G}_j \otimes I(x, y), \quad (5)$$

where I is the palmprint image, $I(x, y)$ is the gray scalar of location (x, y) in the palmprint image, and “ \otimes ” is the convolve operation. All pixels in the image need to convolve with the filter. $R_j(x, y)$ is the filter result of $I(x, y)$ with \tilde{G}_j . The orientations with the most two dominant filter results are extracted as the dominant

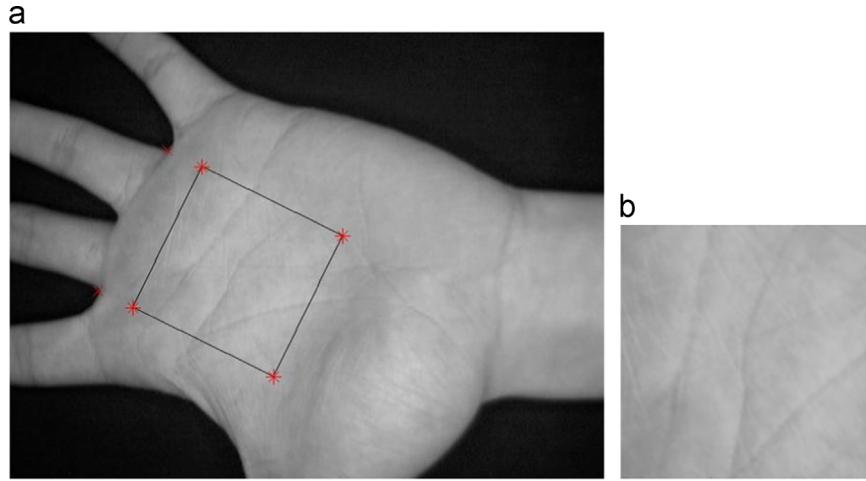


Fig. 6. The ROI extraction of a palmprint image: (a) the input palmprint image and (b) the extracted ROI of the palmprint image.

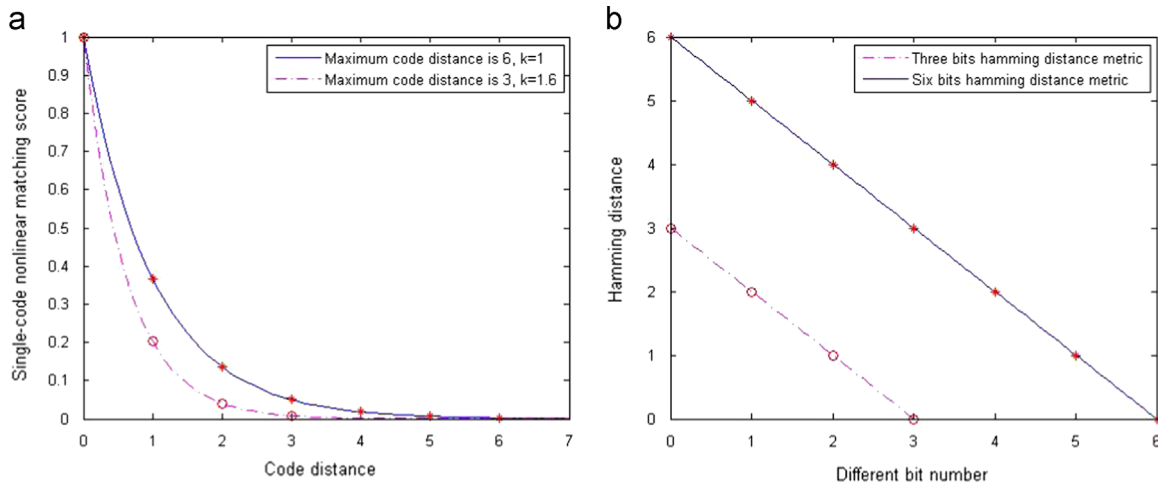


Fig. 7. The matching score obtained using the proposed approach and hamming distance metric: (a) shows the variation of the matching score with the angular distance and (b) shows the variation of the hamming distance with a number of different bits.

orientation features:

$$[O_p(x, y), O_s(x, y)] = \arg \min_{j_1, j_2} R_j(x, y), \quad j = \{0, 1, \dots, n_\theta - 1\}, \quad (6)$$

where j_1 and j_2 are two indices of the two most minimum filter responses. In other words, $O_p(x, y)$ and $O_s(x, y)$ are the two indices of the two most minimum filter responses among $R_j(x, y) (j = 0, 1, \dots, n_\theta - 1)$. We refer to (O_p, O_s) as the double-orientation code (DOC).

4.4. Double-orientation nonlinear matching

In this subsection, the proposed DOC based nonlinear matching scheme is presented. The hamming distance is widely used to calculate the similarity between two palmprint images in coding based approaches. For example, the Palmcode, Fusion code, and Ordinal code approaches all use the hamming distance in the matching stage. The Competitive code approach proposes an angle distance for palmprint recognition, which is equivalent to the sum of three bitwise hamming distances. Guo et al. [33] proposed the unified formula of hamming distance metric. The hamming operation result is 0 if the corresponding bits are the same, otherwise, the result is 1. If two corresponding bits of two series are different, they are referred to as a pair of different bits.

The final matching result is the sum of hamming results of a series of binary codes. So the hamming distance metric is linear with respect to the number: the pairs of different bits of two series.

To increase the discrimination, a nonlinear angular matching score approach is proposed to evaluate the similarity of DOC. In the orientation matching stage, only superior similarity between orientations can acquire a high matching score. When the orientation difference reaches the maximum, the matching score should be a small enough value. The nonlinear matching approach based on “single-orientation code” is defined as

$$ori_score(code_dis) = \frac{1}{e^{k * code_dis}} \quad (7)$$

and

$$code_dis = \min(|O_d - O_t|, n_\theta - |O_d - O_t|), \quad (8)$$

where O_d and O_t are two “single-orientation code”, and k is the parameter. The perfect matching score is 1 when two “single-orientations code” are the same (The code distance $code_dis = 0$). The ori_score should be smaller than ξ , which is a small enough value, when distance of two “single-orientations code” reach the

maximum $n_\theta/2$. In other words,

$$\frac{1}{e^{k*(n_\theta/2)}} < \xi, \tag{9}$$

So

$$k > \frac{2}{n_\theta} \ln \frac{1}{\xi}, \tag{10}$$

where ξ is empirically set as 0.01 in this paper. $k=1.6$ is acceptable when $n_\theta=6$, and $k=1$ is accredited when $n_\theta=12$. Fig. 7(a) shows nonlinear matching scores against the code distance with $n_\theta=12$ and $n_\theta=6$, respectively. Comparatively, Fig. 7(b) depicts the variation of the hamming distance with the number of bits.

For double-orientation code matching score calculation, two crossing matching scores based on code difference are defined as

$$p_1_score(i, j) = ori_score(code_dis_{pp}) + ori_score(code_dis_{ss}), \tag{11}$$

and

$$p_2_score(i, j) = ori_score(code_dis_{ps}) + ori_score(code_dis_{sp}), \tag{12}$$

where

$$code_dis_{\alpha\beta} = \min(|O_\alpha^i - O_\beta^j|, n_\theta - |O_\alpha^i - O_\beta^j|) \quad (\alpha, \beta = p, s). \tag{13}$$

In particular, O_p^i and O_s^i are denoted as DOC of (O_p, O_s) extracted from palmprint image i . $code_dis_{\alpha\beta}$ is the code distance of two pixels from palmprint images i and j . $code_dis_{\alpha\beta}$ is in the range of $\{0, 1, \dots, n_\theta/2\}$. We define the larger of p_1_score and p_2_score as the final matching score of two DOCs:

$$p_score(i, j) = \max(p_1_score(i, j), p_2_score(i, j)). \tag{14}$$

The corresponding DOC based crossing nonlinear matching scores are shown in Table 1. The perfect matching score is 1 when two DOCs are same. If only single sub-orientation-codes of two DOCs are the same, the final matching score will be larger than 0.5, otherwise (two DOC are absolutely different), the final matching score will be equal to or smaller than 0.2019.

The final matching score of two palmprint images is computed as:

$$matching_score(A, B) = \frac{\sum_{i=1}^M \sum_{j=1}^N p_score(i, j)}{2MN}, \tag{15}$$

where M and N are respectively the row number and column number of the palmprint image. The MN is the pixel number of the palmprint image. A and B are two palmprint images. The perfect

matching score is 1 when corresponding DOCs of two palmprint images are same.

The procedure of the palmprint matching score calculation is demonstrated in Fig. 8. DOC is first extracted from each pixel of two palmprint images. Four ori_scores , which are obtained from DOCs of two pixels, are used to calculate the p_1_score and p_2_score . The final $matching_score$ is a normalized summation of the maximum of p_1_score and p_2_score obtained using (16).

5. Experimental results

In this section, a series of experiments was performed to estimate the performance of the proposed approach on three types of popular palmprint databases: including the left and right palmprint database, the multispectral palmprint database [34], and the IITD database [35]. Several state-of-the-art coding based approaches were implemented to compare with the DOC approach.

5.1. Palmprint databases

The left and right palmprint database was provided by the Hong Kong Polytechnic University (PolyU) [34]. It contained 3740 palmprint images collected from 187 different volunteers, where 10 right palmprint images and 10 left palmprint images were captured for each subject. Thus the palmprint database used contained 374 classes and each class had 10 palmprint images. Hereafter the left and right palmprint database is referred to as the PolyU database.

The multispectral palmprint database contained four independent spectral palmprint databases, including the Red spectrum, Green spectrum, Blue spectrum, and Near Infrared (NIR) spectrum palmprint databases [34]. Each of them was collected by PolyU from 500 palms of 250 subjects, including 195 males and 55 females. The age distribution was from 20 to 60 years old. The palmprint images were collected in two separate sessions with a time interval about 9 days. In each session, the subject was asked to provide 6 images for each palm. Therefore, 24 images of each illumination from two palms were collected for each subject. In total, the database contained 6000 images from 500 different palms for one illumination. Thus, each spectral database had 500 classes and each class had 12 palmprint images.

The public IITD palmprint database [35] is a contactless based palmprint database. Images in the IITD database were captured in the indoor environment, and contactless hand images were acquired by a camera with variations in pose, projection, rotation and translation. The main problem of contactless databases lies in the significant intra-class variations resulting from the absence of any contact or guiding surface to restrict such variations. The IITD database consists of 2300 hand images from 230 subjects. Five hand images were captured from each of the left and right hand of each individual in every session. So there were 460 different classes of palmprint images and each class had 5 palmprint images. In addition to the original hand images, the ROI of

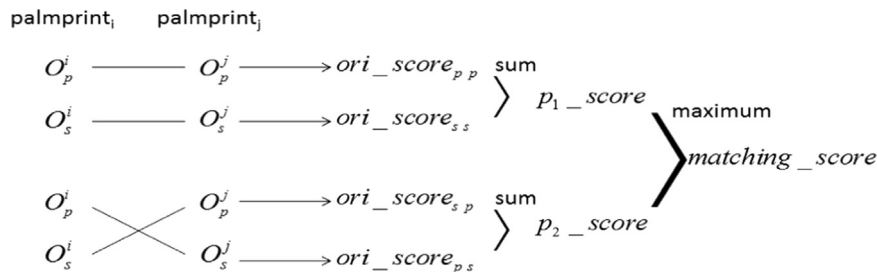


Fig. 8. The procedure to calculate the matching score between DOCs.

Table 1

Crossing nonlinear matching scores of DOC (the maximum code distance is 3).

DOC distance	0	1	2	3
0	1	0.6010	0.5204	0.5041
1	0.6010	0.2019	0.1214	0.1051
2	0.5204	0.1214	0.0408	N/A
3	0.5041	0.1051	N/A	N/A

palmprint images were also available in the database. Fig. 9 shows some palmprint images from three types of palmprint databases.

5.2. Palmprint verification

Verification is a one-to-one comparison which determines whether two samples are from the same class or not. In

palmprint verification, each palmprint image in database is compared with every other samples in database. The matching is counted as genuine matching if both samples are from the same palm, otherwise, the matching is viewed as imposter matching. In the PolyU palmprint database, there are 3740 samples. So the total matching is $3740 \times 3739 / 2 = 6,991,930$, and there are $374 \times 45 = 16,830$ genuine matching (each class has 45 genuine matching) and 6,975,100 imposter matching. There are

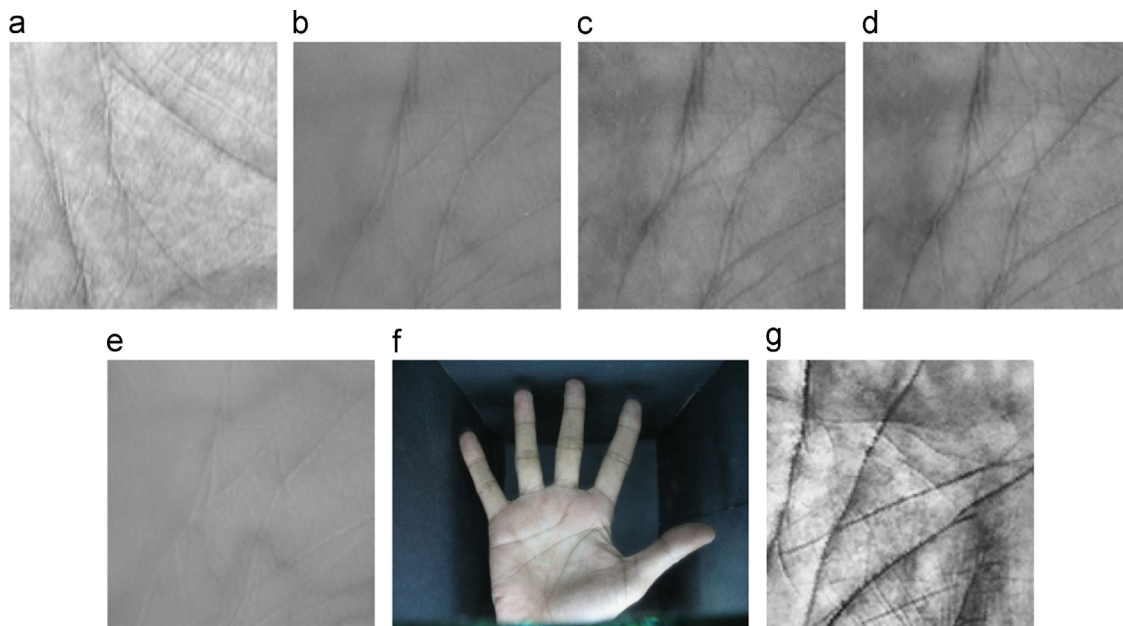


Fig. 9. Examples from these types of palmprint database: (a) is from the PolyU database. (b)–(e) are palmprint images from the Red, Green, Blue, and NIR database, respectively; (f) is a palmprint image from the IITD database; and (g) is the ROI of (f).

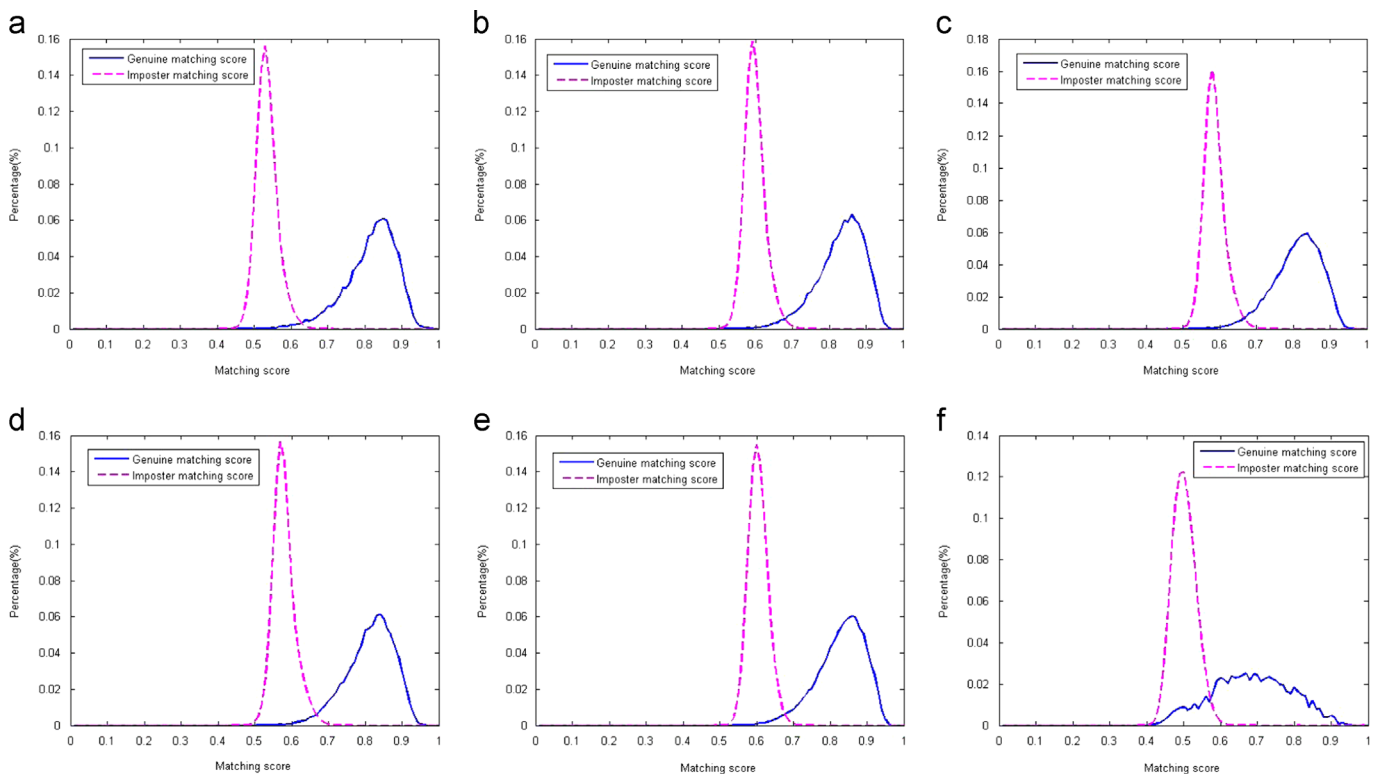


Fig. 10. The matching score distributions obtained using the DOC approach: (a) depicts the distributions of the genuine matching scores and the imposter matching score on PolyU database; (b)–(e) depict distributions of the matching score on Red, Green, Blue, and NIR spectral databases; and (f) plots the matching score distributions on IITD database.

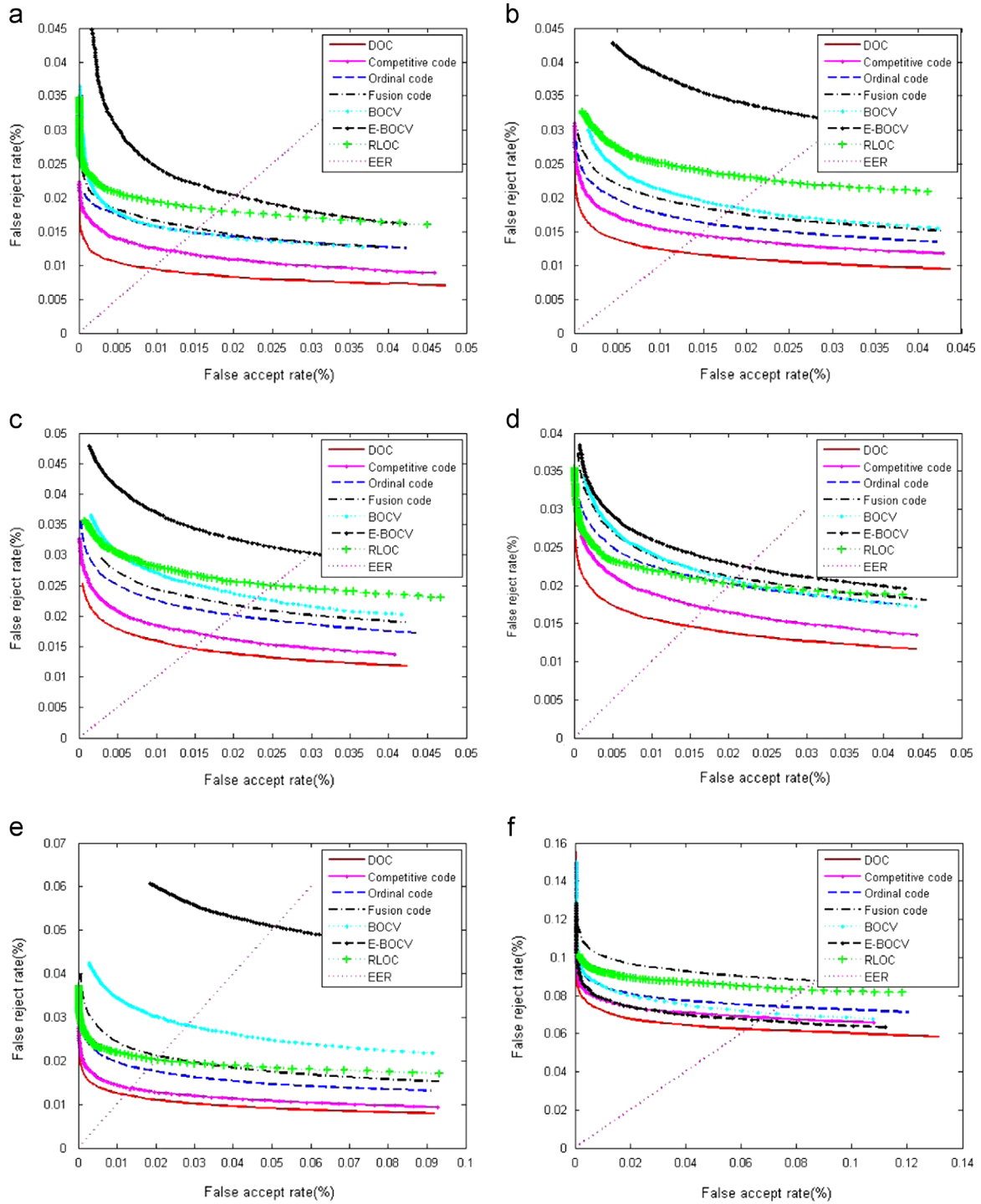


Fig. 11. The ROC curves of different approaches on different types of databases: (a) depicts the ROC curves on PolyU database; (b)–(e) depict ROC curves on Red, Green, Blue and NIR spectral databases; and (f) is the ROC curves on IITD database.

6000 samples in each spectral database. So $6000 \times 5999 / 2 = 17,997,000$ matching totally are performed for each spectral database, and the genuine matching and imposter matching number are 33,000 and 17,964,000. For the IITD database, there are 4600 genuine matching and 100,970 imposter matching. Fig. 10 shows the distributions of genuine matching score and imposter matching score on the PolyU, Red, Green, Blue, NIR, and IITD databases, respectively. It can be observed that the genuine matching score and imposter matching score have highly

separate distributions on both the PolyU and multispectral databases. A linear classifier would be able to distinguish the genuine and imposter classes. The distributions of genuine matching and imposter matching on the IITD database are not as separate as that on the PolyU database. The main reason is that the palmprint images on the IITD database are serious variations in rotation and translation.

In the palmprint verification, False Reject Rate (FRR), False Accept Rate (FAR) and Equal Error Rate (EER) [2] were used to

Table 2
The EERs (%) of different approaches on each palmprint database.

EERs	Comp code	Ordi code	Fuson code	Palm code	BOCV	EBOCV	RLOC	DOC
PolyU	0.0122	0.0150	0.0155	0.0432	0.0149	0.0203	0.0180	0.0092
Red	0.0145	0.0161	0.0179	0.0297	0.0186	0.0313	0.0223	0.0119
Green	0.0168	0.0202	0.0216	0.0507	0.0232	0.0303	0.0249	0.0146
Blue	0.0170	0.0202	0.0212	0.0463	0.0207	0.0225	0.0203	0.0146
NIR	0.0137	0.0180	0.0213	0.0332	0.0284	0.0510	0.0208	0.0121
IITD	0.0696	0.0744	0.0878	0.0933	0.0708	0.0671	0.0826	0.0622

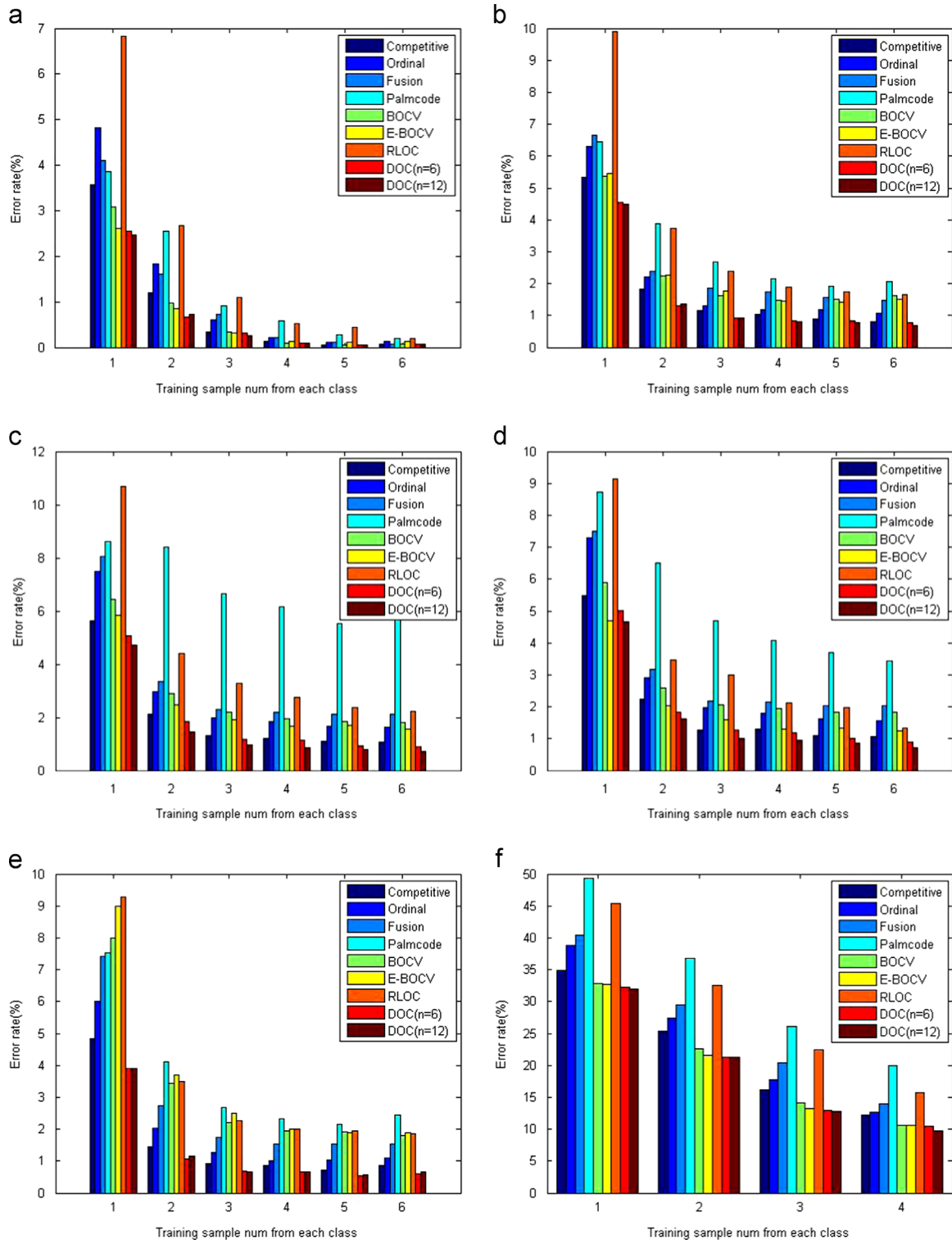


Fig. 12. Palmprint identification error rate: (a) depicts the error rate on PolyU database; (b)–(e) plots the error rate on Red, Green, Blue, and NIR spectral databases; and (f) is the error rates on IITD database.

evaluate the performance of the proposed approach. A matching was counted as correct if the crossing matching score was larger than the threshold, otherwise, the matching was treated as incorrect. For the purpose of analysis, this threshold was considered to be the operating point of FRR, FAR and EER. The Receiver Operating Characteristic (ROC) curve, which is a graph of false reject rate versus false acceptance rate for all possible operating points, was introduced to describe the performance of the palmprint recognition approach. The ROC curves of the DOC approach on three types of palmprint databases are shown in Fig. 11. The ROC curve produced by other approaches, including the Competitive code (Compcode), Ordinal code (Ordicode), Fusion code (Fusncode), RLOC, BOCV, and E-BOCV approaches, are also shown in Fig. 11. The ROC curve of the Palmcode is not plotted in the figure for its FAR and FRR are obviously higher than other approaches. It can be seen that our approach can achieve the lowest FRR against the same FAR on all databases. The corresponding EERs are presented in Table 2. One can see that the DOC approach achieves the smallest EER among all coding approaches.

5.3. Palmprint identification

Identification is a one-against-many comparison process which answers the question of which class of the query sample is. In palmprint identification, the first “TRAIN” palmprint image (s) from each class is/are employed as the training sample and the remaining palmprint images from the testing set. The sample in the testing set is compared with all samples in the training set to produce the DOC matching scores. The testing

sample will be classified to the class of the training sample that produces the highest matching score with the testing sample. Several state-of-the-art coding based approaches, such as the Competitive code, Ordinal code, Fusion code, Palmcode, BOCV, E-BOCV, and RLOC approaches are also implemented to compare with the DOC approach. In the Competitive code approach, the smaller matching score between two competitive code means the more similarity between two samples. So the class of training sample that produce the smallest competitive code matching score will be treated as the class of the testing sample. Other coding based approaches also adopt the same rule as the competitive code approach. The experimental results are shown in Fig. 12, where the error rate is the rate of the number of testing samples that are classified to incorrect class by the number of all testing samples. For the clarity of the presentations, the comparative experimental results with TRAIN=1 and 2 are summarized in Tables 3 and 4, respectively. In addition, the DOC approach using twelve Gabor filters is also implemented.

It can be seen that the proposed DOC approach achieves the lowest identification error rate among all coding approaches on each palmprint database. Generally, the DOC with $n_{\theta}=12$ usually performs better than that with $n_{\theta}=6$. The main reason is that using more filters should extract more accurate orientation feature of the palmprint.

5.4. Comparison with the hamming distance metric

To evaluate the efficiency of the nonlinear matching score scheme, the hamming distance metric is also used to perform double-orientation code matching. The identification error rates obtained by “DOC with hamming metric” approach (TRAIN=1) are listed in Table 5. Compared with the results presented in Table 3, it can be seen that the using of nonlinear matching scheme performs much better than using the hamming distance metric with both $n_{\theta}=6$ and $n_{\theta}=12$. Thus, it can be concluded that the nonlinear matching scheme is suitable for the double-orientation code matching.

5.5. Computational complexity

In this section, we compare the computational complexity of DOC approach with conventional coding based approaches. Since the number of Gabor filters used in DOC ($n_{\theta}=6$) is same as other coding based approaches that use six filters, such as the Competitive code, BOCV and E-BOCV approaches, the convolution computation of DOC is also same as these approaches. Thus, the time cost of code extraction in the DOC approach should be similar with those of the Competitive code, BOCV, and E-BOCV approaches. In the code matching processing of the DOC approach, it should be noted that the distance between two DOC is numerated. So the matching score between two “single-orientation code” just need to be calculated only once, which were listed in Table 1. Thus, the speed of matching score

Table 3
The palmprint identification error rates (%) (train=1).

Err rates	Comp code	Ordi code	Fusn code	Palm code	BOCV	EBOCV	RLOC	DOC ($n_{\theta}=6$)	DOC ($n_{\theta}=12$)
PolyU	3.57	4.81	4.10	3.86	3.09	2.61	6.83	2.55	2.47
Red	5.35	6.31	6.65	6.44	5.36	5.45	9.90	4.55	4.49
Green	5.64	7.49	8.05	8.62	6.44	5.85	10.69	5.07	4.71
Blue	5.47	7.29	7.49	8.73	5.89	4.69	9.13	5.02	4.67
NIR	4.85	6.00	7.40	7.53	8.00	8.98	9.29	3.91	3.89
IITD	34.89	38.86	40.38	49.40	32.88	32.65	45.43	32.23	31.95

Table 4
The palmprint identification error rates (%) (train=2).

Err rates	Comp code	Ordi code	Fusn code	Palm code	BOCV	EBOCV	RLOC	DOC ($n_{\theta}=6$)	DOC ($n_{\theta}=12$)
PolyU	1.20	1.84	1.60	2.54	0.97	0.84	2.67	0.67	0.73
Red	1.82	2.20	2.38	3.88	2.24	2.28	3.74	1.30	1.36
Green	2.14	2.98	3.36	8.42	2.88	2.48	4.40	1.84	1.46
Blue	2.24	2.92	3.18	6.50	2.58	2.02	3.47	1.82	1.62
NIR	1.46	2.04	2.72	4.12	3.44	3.70	3.50	1.06	1.16
IITD	25.36	27.46	29.49	36.74	22.61	21.57	32.54	21.23	21.30

Table 5
The palmprint identification error rates (%) obtained using the hamming distance metric.

Err rates	PolyU	Red	Green	Blue	NIR	IITD
DOC ($n_{\theta}=6$)	2.59	4.61	5.13	5.05	3.97	31.95
DOC ($n_{\theta}=12$)	2.79	4.82	5.24	4.98	4.25	32.87

Table 6
computational costs of different approaches.

Approaches	Code ext	Matching	Approaches	Code ext	Matching
DOC	410 ms	102 ms	BOCV	395 ms	11 ms
Competitive code	383 ms	41 ms	E-BOCV	412 ms	36 ms
Ordinal code	196 ms	67 ms	RLOC	6.680 s	437 ms
Fusion code	40 ms	5 ms	Palmcode	19 ms	3 ms

calculation for “single-orientation code” is also fast. It should be noticed that the DOC consists two “single-orientation code”. So the computational cost in DOC matching stage should be a little more than those of the competitive code, BOCV, and E-BOCV approaches. To facilitate comparison with other coding approaches, several state-of-the-art coding approaches and the DOC approach are implemented by using MATLAB 8.1.0 on a PC with double-core Intel(R) i5-3470 (3.2 GHz), RAM 8.00 GB, and Windows 7.0 operating system. Code extraction and matching between two palmprints are performed for 10 times and the time taken in each phase is shown in Table 6. The code extraction time taken in the DOC approach is about 410 ms, which is comparable to the competitive code, BOCV, and E-BOCV approaches. The matching time of DOC is longer than those of other coding approaches but it is still sufficient for the practical application.

6. Conclusions

Orientation coding based palmprint recognition approaches consists of two main steps: palmprint orientation feature extraction and orientation feature matching. Using a reasonable orientation coding scheme and designing an effective coding based matching algorithm are two important issues in the coding based approaches. This paper analyzes the orientation feature extraction by using discrete filters and proposes a double-orientation code (DOC) extraction approach. The DOC can correctly and robustly represent the palmprint orientation feature. The distance between DOCs is evaluated by using a nonlinear matching score approach. It has been verified that the nonlinear angular matching score approach is more effective than the conventional hamming distance metric in evaluating the similarity of DOC. The proposed DOC approach can achieve significantly higher palmprint verification and identification accuracy than previous state-of-the-art coding approaches.

Conflict of interest

We declare that we have no financial and personal conflict with other people or organizations.

Acknowledgment

This paper is partially supported by the National Natural Science Foundation of China (Grant nos. 61370163, 61233011, 61332011 and 61162001), Shenzhen Municipal Science and Technology Innovation Council (Nos. JCYJ20130329151843309 and JCYJ20140904154630436), Jiangxi Provincial Science and Technology Support Project (20132BBF60083). Thanks to Dr. Edward C. Mignot, Shandong University, for linguistic advice.

References

- [1] A.K. Jain, A. Ross, S. Prabhakar, An introduction to biometric recognition, *IEEE Trans. Circuits Syst. Video Technol.* 14 (1) (2004) 4–20.
- [2] Advanced pattern recognition technologies with applications to biometrics, Medical Information Science Reference, 2009.
- [3] A. Kong, D. Zhang, M. Kamel, A survey of palmprint recognition, *Pattern Recognit.* 42 (7) (2009) 1408–1418.
- [4] Y. Ding, D. Zhuang, K. Wang, A study of hand vein recognition method, in: *IEEE International Conference on Mechatronics and Automation 2005*, vol. 4, IEEE, 2005, pp. 2106–2110.
- [5] Q. Dai, N. Bi, D. Huang, et al., M-band wavelets application to palmprint recognition based on texture features, in: *International Conference on Image Processing*, 2004, pp. 893–896.
- [6] J. Gui, W. Jia, L. Zhu, et al., Locality preserving discriminant projections for face and palmprint recognition, *Neurocomputing* 73 (13) (2010) 2696–2707.
- [7] S. Ribaric, I. Fratric, A biometric identification system based on eigenpalm and eigenfinger features, *IEEE Trans. Pattern Anal. Mach. Intell.* 27 (11) (2005) 1698–1709.
- [8] K.H. Cheung, A. Kong, D. Zhang, et al. Does eigenpalm work? A system and evaluation perspective, in: *Proceedings of the 18th International Conference on Pattern Recognition 2006. ICPR 2006*, IEEE, vol. 4, 2006, pp. 445–448.
- [9] H. Sang, W. Yuan, Z. Zhang, Research of palmprint recognition based on 2DPCA, *ISNN 2* (2009) 831–838.
- [10] A. Kong, D. Zhang, M. Kamel, Palmprint identification using feature-level fusion, *Pattern Recognit.* 39 (3) (2006) 478–487.
- [11] R. Chu, S. Liao, Y. Han, et al. Fusion of face and palmprint for personal identification based on ordinal, *(CVPR)* 2007, pp. 1–2.
- [12] E. Liu, A.K. Jain, J. Tian, A coarse to fine minutiae-based latent palmprint matching, *IEEE Trans. Pattern Anal. Mach. Intell.* 35 (10) (2013) 2307–2322.
- [13] D.S. Huang, W. Jia, D. Zhang, Palmprint verification based on principal lines, *Pattern Recognit.* 41 (4) (2008) 1316–1328.
- [14] J. Dai, J. Feng, J. Zhou, Robust and efficient ridge-based palmprint matching, *IEEE Trans. Pattern Anal. Mach. Intell.* 34 (8) (2012) 1618–1632.
- [15] A. Morales, M.A. ferre, A. Kumar, Towards contactless palmprint authentication, *IET Comput. Vis.* 5 (2011) 407–416.
- [16] E. Liu, A.K. Jain, J. Tian, A coarse to fine minutiae-based latent palmprint matching, *IEEE Trans. Pattern Anal. Mach. Intell.* 35 (10) (2013) 2307–2322.
- [17] W. Li, L. Zhang, D. Zhang, G. Lu, J. Yan, Efficient joint 2D and 3D palmprint matching with alignment refinement, *CVPR* (2010) 795–801.
- [18] D. Zhang, Z. Guo, G. Lu, L. Zhang, W. Zuo, An online system of multi-spectral palmprint verification, *IEEE Trans. Instrum. Meas.* 59 (2) (2010) 480–490.
- [19] L. Zhang, M. Yang, X. Feng, Sparse representation or collaborative representation: which helps face recognition, *IEEE Int. Conf. Comput. Vis.* (2011) 471–478.
- [20] Y. Xu, D. Zhang, J. Yang, J.Y. Yang, A. two-phase test, sample sparse representation method for use with face recognition, *IEEE Trans. Circuits Syst. Video Technol.* 21 (9) (2011) 1255–1262.
- [21] Guo Z., Wu G., Chen Q., et al. Palmprint recognition by a two-phase test sample sparse representation, in: *Proceedings of the 2011 International Conference on Hand-Based Biometrics (ICHB)*, IEEE, 2011, pp. 1–4.
- [22] D. Zhang, W.K. Kong, J. You, L.M. Wong, Online palmprint identification, *IEEE Trans. Pattern Anal. Mach. Intell.* 25 (9) (2003) 1041–1050.
- [23] A.W.K. Kong, D. Zhang, Competitive coding scheme for palmprint verification, *ICPR 1* (2004) 520–523.
- [24] W. Jia, D. Huang, D. Zhang, Palmprint verification based on robust line orientation code, *Pattern Recognit.* 41 (2008) 1504–1513.
- [25] W. Zuo, Z. Lin, Z. Guo, D. Zhang, The multiscale competitive code via sparse representation for palmprint verification, *CVPR* (2010) 2265–2272.
- [26] A. Kong, D. Zhang, M. Kamel, Palmprint identification using feature-level fusion, *Pattern Recognit.* 39 (2006) 478–487.
- [27] Z. Sun, T. Tan, Y. Wang, S. Li, Ordinal palmprint representation for personal identification, *Comput. Vis. Pattern Recognit.* 1 (2005) 279–284.
- [28] Z. Guo, D. Zhang, L. Zhang, W. Zuo, Palmprint verification using binary orientation co-occurrence vector, *Pattern Recognit. Lett.* 30 (2009) 1219–1227.
- [29] L. Zhang, H. Li, J. Niu, Fragile bits in palmprint recognition, *IEEE signal Process. Lett.* 19 (10) (2012) 663–666;
- [30] L. Zhang, H. Li, Encoding local image patterns using Riesz transforms: with application to palmprint and finger-knuckle-print recognition, *Image Vis. Comput.* 30 (2012) 1043–1051.
- [31] J.G. Gaugman, High confidence visual recognition of persons by a test of statistical independence, *IEEE Trans. Pattern Anal. Mach. Intell.* 15 (11) (1993) 1148–1161.
- [32] J.H. van Deemter, J.M.H. Du Buf, Simultaneous detection of lines and edges using compound Gabor filters, *Pattern Recognit. Artif. Intell.* 14 (2000) 757–777.
- [33] F. Xue, W. Zuo, K. Wang, A performance evaluation of filter design and coding schemes for palmprint recognition, in: *Proceedings of the 19th International Conference on Pattern Recognition, ICPR 2008*, 2008, pp. 1–4.
- [34] Z. Guo, W. Zuo, L. Zhang, D. Zhang, A unified distance measurement for orientation coding in palmprint verification, *Neurocomputing* 73 (2010) 944–950.
- [35] PolyU palmprint database, Multispectral palmprint database, (<http://www.comp.polyu.edu.hk/~biometrics/>).
- [36] IITD Touchless Palmprint Database(version1.0), (http://www4.comp.polyu.edu.hk/~csajaykr/IITD/Database_Palm.htm).

Lunke Fei received the B.S. and M.S. degree in computer science and technology from East China Jiaotong University, China, in 2004 and 2007. He is currently pursuing the Ph.D. degree in computer science and technology at Shenzhen Graduate School, Harbin Institute of Technology, Shenzhen, China. His current research interests include pattern recognition and biometrics.

Yong Xu received the B.S. and M.S. degrees in 1994 and 1997, respectively, and the Ph.D. degree in pattern recognition and intelligence system from the Nanjing University of Science and Technology, Nanjing, China, in 2005. Currently, he is with the Bio-Computing Research Center, Shenzhen Graduate School, Harbin Institute of Technology, Shenzhen, China. His current research interests include pattern recognition, biometrics, bioinformatics, machine learning, image processing, and video analysis.

Wenliang Tang received the M.S. degree in computer application technology from Sichuan University, Chengdu, China, in 1999. Currently, he is with the School of Software, East China Jiaotong University, Nanchang, China. He is also a visiting scholar of University of California, Los Angeles now. His research interests include pattern recognition and WSN technology.

David Zhang graduated in computer science from Peking University. He received his M.Sc. in computer science in 1982 and Ph.D. in 1985 from the Harbin Institute of Technology (HIT). From 1986 to 1988, he was a postdoctoral fellow at Tsinghua University and then an associate professor at the Academia Sinca, Beijing. In 1994, he received his second Ph.D. in electrical and computer engineering from the University of Waterloo, Ontario, Canada. Currently, he is the Head, Department of Computing, and a chair professor at the Hong Kong Polytechnic University, where he is the founding director of the Biometrics Technology Centre (UGC/CRC) supported by the Hong Kong SAR government in 1998. He also serves as visiting chair professor in Tsinghua University, and Adjunct Professor in Peking University, Shanghai Jiao Tong University, HIT and the University of Waterloo. He is the founder and editor-in-chief of the International Journal of Image and Graphics (IJIG); book editor of the Springer International Series on Biometrics (SISB); organizer of the International Conference on Biometrics Authentication (ICBA); Associate Editor of more than 10 international journals, including IEEE Transactions and Pattern Recognition; and the author of more than 10 books and 200 journal papers. Professor Zhang is a Croucher senior research fellow, distinguished speaker of the IEEE Computer Society, and fellow of both IEEE and IAPR.